



MONITORING OF HIGH FREQUENCY VIBRATION SIGNAL USING FBG DEMODULATION

Sang-Oh Park*, Zi-Jing Wong*, Sang-Wuk Park*, Chun-Gon Kim*

*Dep. of Aerospace Engineering, Korea Advanced Institute of Science and Technology
373-1, Kuseong-dong, Yuseong-gu, Daejeon, 305-701, Korea

Keywords: *fiber Bragg grating sensor, structural health monitoring, high frequency vibration*

Abstract

For the monitoring of the high frequency vibration signal, a fiber Bragg grating (FBG) demodulation system was proposed. This demodulator, based on a FBG receiver could detect high-frequency signal such as vibration signal using intensity demodulation. The FBG demodulation system has several merits; low cost needed to construct the system, unnecessary of other stabilization methods, and capability of multiplexed measurement. In this study, the performance verification of FBG demodulation system was carried out. Several tests were conducted to determine the system's sensitivity and resolution. Then the FBG demodulation system was applied for using the health monitoring of the composite joint specimens using an active inspection system.

1 Introduction

Composites have many advantages such as high specific strength, stiffness, corrosion resistance in harsh environment, and the ability to sustain extreme temperature. Therefore the interests in composites have been increasing, and composite structural elements are widely used in making various components for automotive, aerospace, marine, and civil structures [1]. However, the fracture mechanism of composites is very complex under impact and internal damages are not easily detected compared to homogeneous metallic materials. Hence for the reliability of structures, the structural health monitoring technology is necessary to be integrated in the composite structures.

Recently, as the integrated sensing part of composite structures, fiber optic sensors (FOSs) have been widely used due to their convenience of embedment without causing much mechanical defects in structures. Especially, fiber Bragg grating

sensor (FBG) has the most excellent ability in multiplexing among various FOSs. Whenever the grating is exposed to external perturbations, the Bragg wavelength changes. By measuring the wavelength shift, we can calculate the physical properties such as strain and temperature. However, the method typically used to measure the wavelength change directly cannot monitor high frequency vibration signal accurately such as acoustic emission signal.

In recent years, many efforts have been undertaken to develop built-in structural health monitoring systems that can generate Lamb wave modes which are sensitive to damage by using transducers of various types, including transducer arrays [2–4]. The application of Lamb waves to the health monitoring of composite materials began in the late 1980s. Since then, a wide range of studies has been conducted for composite plates [5–8].

In this study, the FBG demodulation system was composed, using the intensity demodulation scheme. The performance verification of FBG demodulation system was carried out under high frequency vibration condition. Several tests were conducted for the determination of its sensitivity and resolution. Then FBG demodulation system was utilized in conjunction with the active sensing method to monitor a series of composite joint specimen.

2 Fabrication of FBG sensors

There are many ways for FBG sensors. Fabrication method using a phase mask [9] is currently the most prevalently employed technique because it has an advantage of fabrication simplicity and hence suitable for mass production. A commercial phase mask generally has a specific grating length of 10 mm, and thus the gage length of normally fabricated FBGs is also limited to 10 mm. In this fabrication setup, an Al screen and a

translation stage were used to make various grating lengths of FBGs. A KrF excimer laser (ASX-750, MPB Co., Canada) was used as the UV light source. The setup for the fabrication process of FBGs is shown in Fig. 1.

The photosensitive optical fiber (PS1250/1500, Fibercore Co., United Kingdom) was made to the reflectivity of 90 % (10 dB) in gage length of 10 mm by a phase mask (IBSEN Co., Denmark). The gage length of 5 mm was made by covering half of the phase mask using an Al screen. For the other gage lengths of more than 10 mm, after making gage length of 10 mm with 10 dB by the exposure to the UV interference for 15 seconds, the optical fiber was shifted 10 mm using the translation stage and exposed again to the UV for 15 seconds.

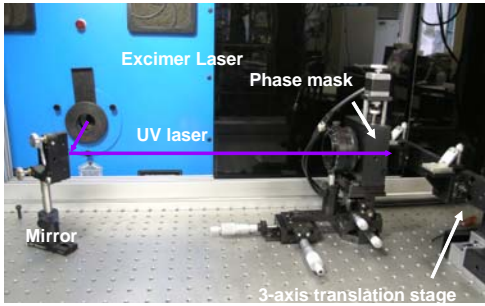


Fig. 1 Fabrication of FBG sensor.

3 FBG sensor systems

3.1 Principle of measurement

A fiber Bragg grating is unique for the periodic changes of the refractive index property within the fiber gage length. The light of a specific Bragg wavelength, which is determined by the Bragg condition, is reflected at the Bragg grating part while lights with the other wavelengths pass through it. In Eq. (1), the Bragg wavelength is expressed as a multiple of the effective refractive index of the Bragg condition grating period [10]. Whenever grating is exposed to external perturbations, the Bragg period is either elongated or contracted, therefore resulting in the change of Bragg wavelength.

$$\lambda_B = 2n_e \Lambda \quad (1)$$

Fig. 2 shows the schematic of FBG sensor system to obtain the acoustic emission signal during the fracture of the composites.

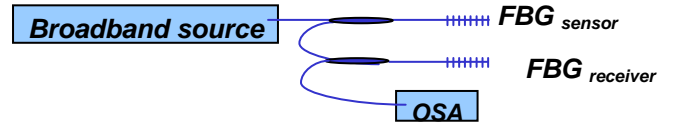


Fig. 2 FBG dual demodulation system.

FBG sensor and receiver were manufactured to the same reflective wavelength, the same gage length of 10 mm and the same reflectivity of 10 dB. Then the full spectrum of the reflective wavelength could be received. If the Bragg wavelength of a FBG sensor is shifted by a vibration, the vibration can be expressed by the intensity variation using FBG receiver as shown in Fig. 3. Eq. (2) is the reflectivity of FBG sensor [11], where $\Delta\beta$ is the differential propagation constant written as $2\pi n_e [(1/\lambda) - (1/\lambda_B)]$, s is $(\Omega^2 - \Delta\beta^2)^{1/2}$, and Ω is a coupling coefficient.

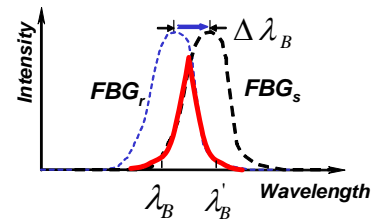


Fig. 3 Principle of FBG self demodulation.

$$R(\lambda) = \frac{|\Omega|^2 \sinh^2(sL)}{\Delta\beta^2 \sinh^2(sL) + s^2 \cosh^2(sL)} \quad (2)$$

The output voltages were measured after shifting the wavelength in the FBG sensor for 0.02 nm using micro-positioner. Fig. 4 shows the intensity variation of the FBG demodulation system that is similar to the reflective spectrum of FBG sensor.

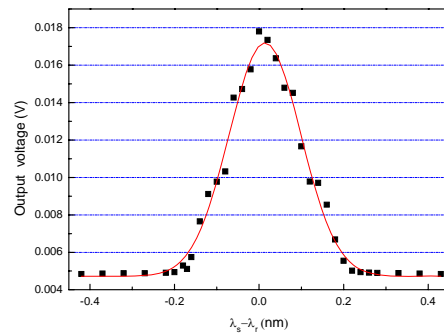


Fig. 4 Output voltage at each wavelength shift.

3.2 Measurement of sensitivity for vibration

The performance verification of FBG demodulation system to determine the sensitivity and resolution was carried out. The signal to noise ratio (S/N ratio) was calculated from the power spectral density (PSD) which shows the distribution for a special frequency of an input signal, shown in the Eq. (3). This result was the root mean square (RMS) value of the strain acquired by FBG sensor. The noise level could be computed from applied strain and S/N ratio, and the noise is RMS of the noise level, as shown in Eq. (4). Sensitivity and resolution of the sensor can be calculated using sampling frequency and bandwidth as displayed in Eq. (5) and (6) respectively.

$$S/N = 10 \times \log \left(\frac{\varepsilon_{FBG,rms}^2}{Noise^2} \right) \quad (3)$$

$$Noise(\varepsilon_{rms}) = \frac{\varepsilon_{FBG,rms}}{10^{\frac{S/N}{20}}} \quad (4)$$

$$sensitivity(\varepsilon_{rms} / \sqrt{Hz}) = \frac{\varepsilon_{FBG,rms}}{10^{\frac{S/N}{20}}} / \sqrt{df} \quad (5)$$

$$resolution(\varepsilon_{rms}) = sensitivity(\varepsilon_{rms} / \sqrt{Hz}) \times \sqrt{BW} \quad (6)$$

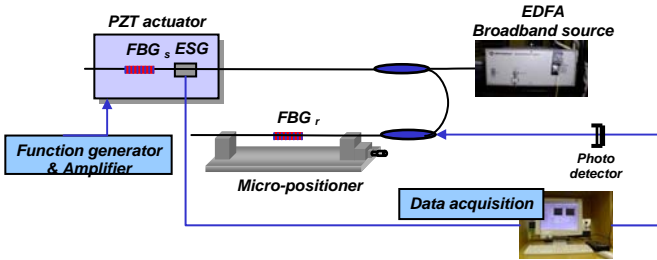


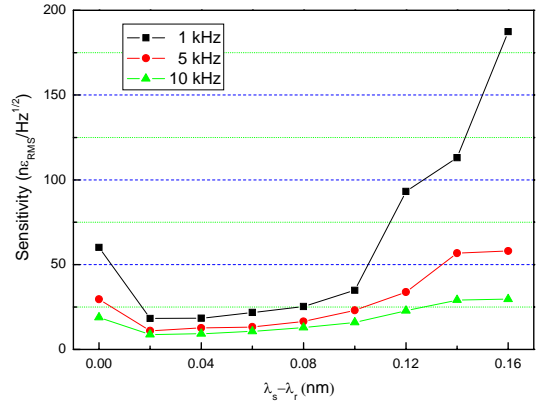
Fig. 5 FBG vibration sensor system for the sensitivity evaluation.

The experimental setup for vibration performance test is shown in the Fig. 5. The FBG sensor and strain gage were attached on PZT actuator (C-82, Fuji Ceramics co., Japan) by an adhesive (cyanoacrylate TML co., Japan). The PZT actuator was connected to the function generator (AFG 320, Tektronix, Inc. Japan). The data of strain gage was used as the reference data to compare with the FBG result.

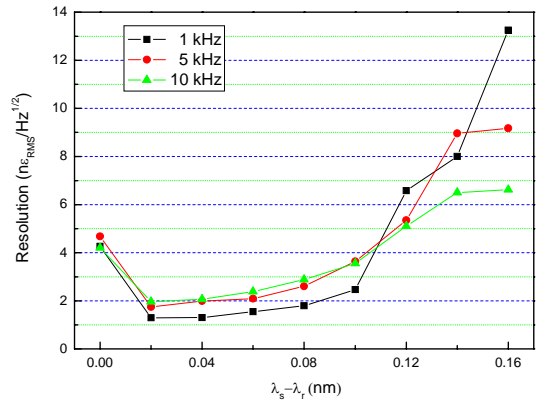
In order to verify the performance, FBG sensors which have 0.02 nm shift of wavelength as compared to the refractive wavelength of FBG receiver were vibrated with different oscillating

frequency (1, 5, 10 kHz). Actuating voltage was applied to Piezo ceramic actuator with $-10 \sim 10$ V range. From Eq. (3) ~ (6), signal to noise ratio, sensitivity, and resolution were calculated.

The strain of PZT changed to $3.15 \mu\epsilon$ at 1kHz, $3.37 \mu\epsilon$ at 5kHz, and $3.87 \mu\epsilon$ at 10kHz for +10 V. The S/N ratio were 41.99 dB(1 kHz), 39.34 dB(5 kHz), and 38.25 dB(10 kHz) respectively for 0.2 nm shift between wavelengths of FBGs (FBG sensor) and FBGr (FBG receiver). The S/N ratio of more than 30 dB was obtain for below 0.1 nm shift. The sensitivity and resolution were $18.3 n\varepsilon_{rms} / \sqrt{Hz}$, $1.2951 n\varepsilon_{rms}$ (1 kHz), $11.0 n\varepsilon_{rms} / \sqrt{Hz}$, $1.7431 n\varepsilon_{rms}$ (5 kHz), $8.8 n\varepsilon_{rms} / \sqrt{Hz}$, $1.9670 n\varepsilon_{rms}$ (10 kHz) for 0.2 nm shift between wavelengths of FBGs and FBGr. The sensitivity and resolution also increased substantially and the performance of this system depressed over 0.1 nm shift between wavelengths of FBGs and FBGr.

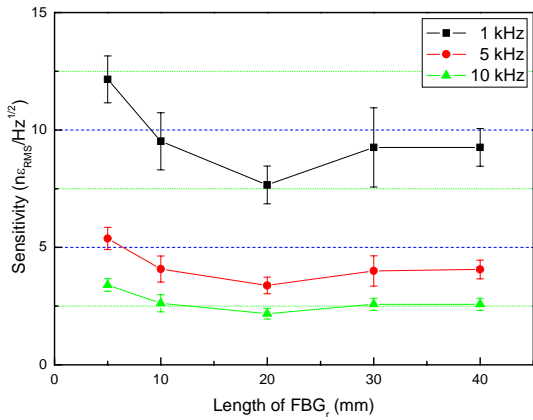


(a) Sensitivity.

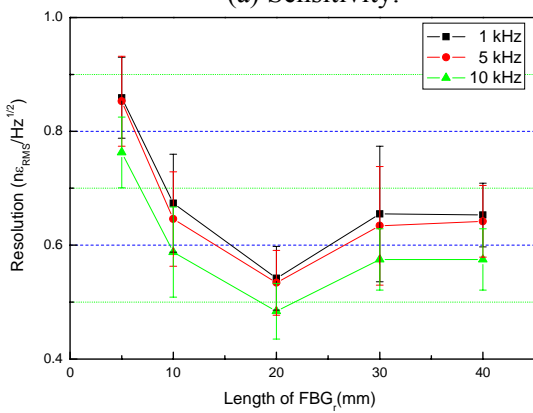


(b) Resolution.

Fig. 6 Vibration performance test with wavelength shift at 10 nm FBG receiver.



(a) Sensitivity.



(b) Resolution.

Fig. 7 Vibration performance test with different gage length of FBG receiver.

The results for experiments with FBG sensor of 10 mm gage length are shown in Fig. 6. As the vibration frequency increases, the sensitivity decreases and the resolution increases for below 0.1 nm wavelength differenc. As the shift of the Bragg wavelength increases, the performances of sensitivity and resolution decline except the case of zero shift.

Fig. 7 shows the change of sensitivity and resolution according to the gage length of FBGr. As the gage length of FBGr increased, the performance of the sensor system was also improved. It was assumed that the sensitivity and resolution of this system could be better by increasing the gage length of FBGr.

4 Application

4.1 Specimen

There are two kinds of joining methods for composite structures. One is mechanical fastening and the other is adhesive bonding. Adhesively

bonded joint is more efficient than mechanical fastening joint because the load transfer is more uniformly carried through larger area. Recently, many composite structures have been made by using the bonded joint.

In this study, 5 composite joint specimens with different debonding length were used. These specimens were made of Graphite/Epoxy prepregs (CU-125NS, Hankook fiber glass co., Korea), using autoclave curing. The 0° angle refers to the horizontal direction (right and left) of the specimen, and the properties of laminates were shown in Table 1. The specimens were fabricated to have the same shape but with different debonding lengths; 0 mm, 20 mm, 40 mm, 60 mm, and 80 mm by after-curing in the autoclave, as shown in the Fig. 8.

Table 1 Stiffness properties of CU-125NS lamina

E_1	E_2, E_3	G_{12}, G_{13}	G_{23}	ν_{12}, ν_{13}	ν_{23}
135.4 GPa	9.6 GPa	4.8 GPa	3.2 GPa	0.31	0.52

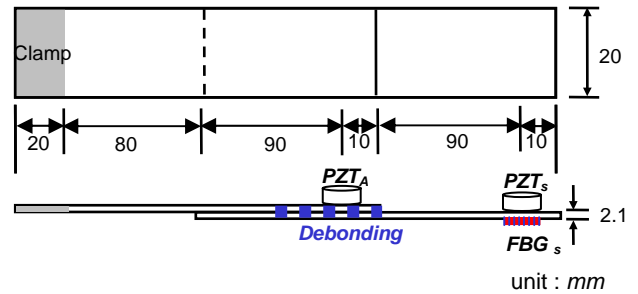


Fig. 8 Geometry and dimension of the composite joint specimens.

4.2 Experimental setup

For the application of health monitoring in an active inspecting system, FBG sensors with FBG demodulation system and PZTs with a circular shape (C6, Fuji Ceramics) were used. FBG sensors and PZTs were bonded to the surface of the composite joint specimens using cyanoacrylate adhesive, as shown in the Fig. 9. PZTs were used as transmitter or sensor since they can exhibit both actuating and sensing behavior. FBG sensors with the gage length of 5 mm were located in the same position with PZT

MONITORING OF HIGH FREQUENCY VIBRATION SIGNAL USING FBG DEMODULATION

sensors. The PZTs were 5 mm in diameter and 2 mm thick. The FBG sensor and PZT sensor were placed in the intervals of 100 mm from the PZT transmitter which was excited using a function generator. The received signals were collected with an oscilloscope (TDS3014, Tektronix, Inc., Japan) and then transferred to a PC for data processing through a GPIB interface. The function generator also transferred a trigger signal to the oscilloscope to set the initial data recording time. The experimental test setup is shown in Fig. 9. FBG receiver with gage length of 20 mm was used for the experiment.

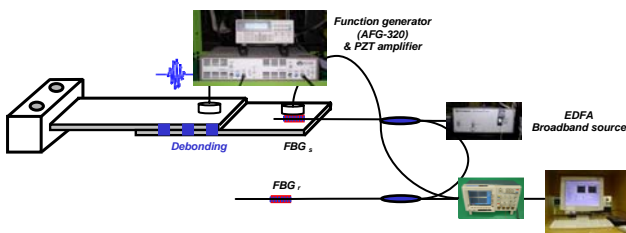


Fig. 9 Experimental setup for application to joint specimen.

4.3 Procedure

First, the response test on the joint specimen with no debonding was carried out. The applied input signals were five cycles sinusoidal tone burst from 20 kHz to 100 kHz. The received signals were acquired at a sampling rate of 10 MS/s by the digital oscilloscope, which averaged 256 samples in order to improve the S/N ratio. As shown in the Fig. 10, the signal responses of FBG sensor and PZT sensor varied with the frequency change. As the frequency increased, the response of FBG was low and that of PZT was high. However, both the signal responses were satisfactory at actuating frequency of around 50 kHz. Therefore, 50 kHz input signal was chosen for the active sensing application.

The input signals were five cycles 50 kHz sinusoidal tone burst to detect the debonding of the joint specimen. The received signals were acquired at a sampling rate of 10 MS/s by the digital oscilloscope with averaged 256 samples. Then, lamb wave with one cycle 300 kHz sinusoidal tone burst were excited to measure the debonding length. Debonding length can be calculated by using the time difference between the input and detected signals. The signals were obtained at a sampling rate of 100MS/s.

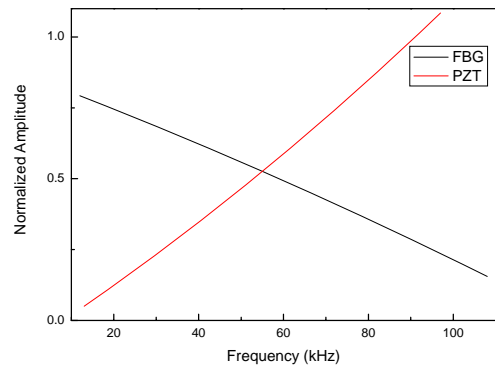
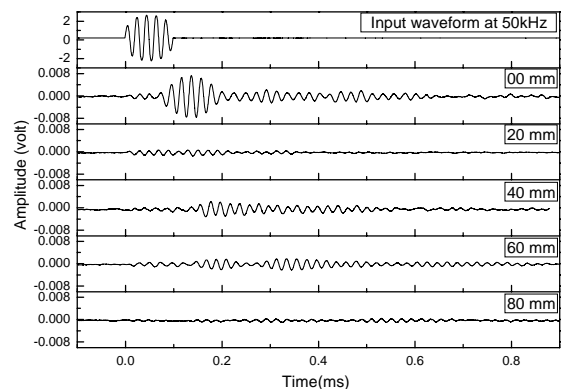


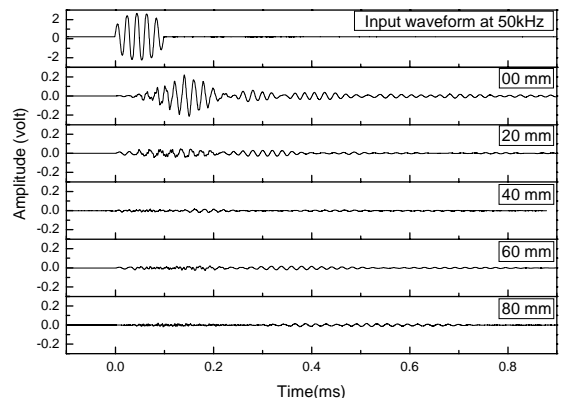
Fig. 10 Signal response with frequency change.

4.4 Results

Fig. 11 shows that the signal of FBG sensor and PZT sensor were similar and attenuated in the debonded joint dramatically. The signal at a low frequency was dominant in an antisymmetric mode A_0 which can't easily change its path compared to a symmetrical mode S_0 . Therefore it was conformed the the signal at low frequency was not suited to measure the debonding length of the joint.



(a) FBG sensor.



(b) PZT sensor.

Fig. 11 Signal response at 50 kHz frequency.

On the other hand, Fig. 12 shows the time difference in the first response peak with difference debonding length cases. The time difference increased accordance in debonding length increment. The time differences were 14.38 μ s, 17.11 μ s, 20.62 μ s, 25.17 μ s, and 30.09 μ s respectively for each debonding length from the positive peak of input waveform. The velocity of s mode was almost 7529.8 m/s.

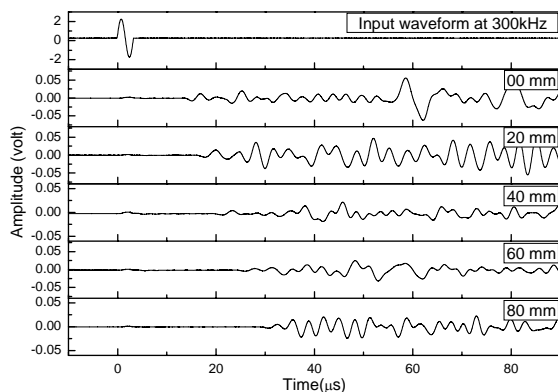


Fig. 12 Signal response of PZT sensor at 300 kHz frequency.

5 Conclusions

For the monitoring of the high frequency vibration signal, a FBG demodulation system was proposed. This system using an FBG receiver could detect high frequency signal such as composite fracture occurrence using intensity demodulation. The FBG demodulation system has several merits; low cost required to construct the system, unnecessary of other stabilization methods, and capability of multiplexed measurement.

In this study, the performance verification of FBG demodulation system was carried out. Several tests were conducted to determine the sensitivity and resolution. For application of health monitoring in an active inspecting system, FBG sensors with FBG demodulation was used and the result were compared with those of PZT sensors.

Acknowledgement

The present work was supported by the Korea Science and Engineering Foundation (project No. R01-2004-000-11009-0). This support is gratefully acknowledged.

References

- [1] R. F. Gibson, "Principles of Composite Material Mechanics", McGraw-Hill, Inc., 13, 1994.
- [2] Liu T, Veidt M, Kitipornchai S., "Single mode Lamb wave in composite laminated plates generated by piezoelectric transducer," *Composites and Structures*, Vol 58, pp. 381–396, 2002.
- [3] Giurgiutiu V, Bao J, Zhao W., "Active sensor propagation health monitoring of beam and plate structures," *Proceeding of the SPIE 8th international symposium on smart structures and material*, 2001.
- [4] Anthony G, Gordon H, et al. "Generation and reception of ultrasonic guided waves in composite plates using conformable piezoelectric transmitters and optical-fiber detectors," *IEEE Trans Ultrason Ferroelectrics Frequency Control*, Vol. 46, No. 1, pp. 72–81, 1999.
- [5] Ye L, Su Z., "A damage identification technique for CF/EP composite laminates using distributed piezoelectric transducers," *Composites and Structures*, Vol. 57, pp. 465–71, 2002.
- [6] Kessler SS, Spearing SM, Soutis C., "Damage detection in composite materials using Lamb wave methods," *Smart Materials and Structures*, Vol. 11, pp.269–278, 2002.
- [7] Lemistre M, Balageas D., "Structural health monitoring system based on diffracted Lamb wave analysis by multiresolution processing," *Smart Materials and Structures*, Vol. 10, pp. 504–11, 2001.
- [8] Sohn H, Park G, Jeannette RW, Nathan PL. "Wavelet-based active sensing for delamination detection in composite structures," *Smart Materials and Structures*, Vol. 13, pp. 153–160, 2004.
- [9] K. O. Hill, B. Malo and F. Bilodeau, et al., "Bragg gratings fabricated in monomode photosensitive optical fiber by UV exposure through a phase mask," *Applied Physics Letters*, Vol. 62, No. 10, pp. 1035–1037, 1993.
- [10] E. Udd, "Fiber Optic Smart Structures", John Wiley and Sons, 1995.
- [11] A. B. L. Ribeiro, L. A. Ferreira, and J. L. Santos, "Analysis of the reflective matched fiber Bragg grating sensing interrogation scheme," *Applied Physics Letters*, Vol. 36, No. 4, pp. 934–939, 1997.